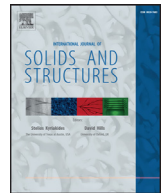




Contents lists available at ScienceDirect

International Journal of Solids and Structures

journal homepage: www.elsevier.com/locate/ijsolstr

On weak and strong contact force networks in granular materials

N.P. Kruyt*

Department of Mechanical Engineering, University of Twente, P.O. Box 217, 7500 AE Enschede, The Netherlands

ARTICLE INFO

Article history:

Received 8 October 2015

Revised 28 January 2016

Available online xxx

Keywords:

Granular materials

Micromechanics

Stress transmission

Contact force networks

ABSTRACT

In an influential study on the micromechanical origin of stress transmission in granular materials, Radjai et al. (1998) have proposed a division of the network of interparticle contacts into 'weak' and 'strong' contacts. This division is based on a comparison of the force at contacts with the average (over all contacts) force. They observed, from the results of a two-dimensional computer simulation of the behaviour of a system of particles, that the shear stress of the granular material is mainly carried by the strong contacts and that the anisotropy in the orientational distribution of the weak contacts is in the direction perpendicular to that of the full contact network.

These findings are analytically predicted here in a qualitative sense, within a statistical framework that is based on a simple, self-similar expression for the conditional probability function for the normal force at contacts with given contact orientation.

An alternative definition of weak and strong contacts is proposed here, in which the division of the contacts is based on a comparison of the force at contacts with the average force corresponding to the contact orientation. Contrary to the finding based on the definition of weak and strong contacts by Radjai et al. (1998), with this alternative definition the pressure and the shear stress are (almost) equally carried by the weak contact network.

© 2016 Elsevier Ltd. All rights reserved.

1. Introduction

Granular materials are systems consisting of a large number of particles with frictional interactions. Macroscopically, these systems exhibit a shear strength that is pressure dependent. Conventionally, this is described by the Mohr–Coulomb yield criterion at the macroscopic, continuum scale.

For granular materials consisting of stiff particles, the microscopic scale of interest is that of particles and interparticle contacts. Particles interact at these contacts through contact forces. In micromechanics of quasi-static deformation of granular materials, relationships are investigated between micro-scale characteristics of particles and contacts and macroscopic characteristics of stress and strain.

An important characteristic at the microscopic scale of contacts is the distribution of contact orientations. Computer simulations and results from experiments have demonstrated that this distribution is in general anisotropic (for example Biarez and Wiendieck, 1963; Oda, 1972a, 1972b, 1972c; Rothenburg and Bathurst, 1989), either due to the method of sample preparation (inherent anisotropy) or due to deformation (induced anisotropy).

The micromechanical origin of stress transmission in granular materials has been investigated from a number of viewpoints. Ex-

periments using photo-elastic materials have demonstrated the importance of anisotropy at the microscopic scale in the distribution of contact orientations (for example Biarez and Wiendieck, 1963; de Josselin de Jong and Verruijt, 1969; Drescher and de Josselin de Jong, 1972; Oda, 1972a, 1972b, 1972c; Majmudar and Behringer, 2005). Rothenburg and Bathurst (1989) developed the stress–force–fabric relationship, which gives a quantitative relationship between macroscopic shear strength and microscopic anisotropies in contact orientations and in contact force distributions. Subsequent further developments of stress–force–fabric relationships have been reported by Quadfel and Rothenburg (2001), Li and Yu (2013) and Azéma et al. (2013). A different, influential viewpoint on stress transmission in granular materials has been proposed by Radjai et al. (1998). This viewpoint forms the focus of the current study.

Radjai et al. (1998) have proposed to divide the set of interparticle contacts into two disjoint subsets, the 'weak' and the 'strong' contact networks. The weak contacts are defined as those contacts c at which the normal force f_n^c is smaller than a threshold value that depends on the average (over all contacts) normal force \bar{F} . For strong contacts c , the normal force f_n^c is larger than the average normal force \bar{F} . Thus

$$\text{Weak contacts : } f_n^c \leq \xi \bar{F} \quad \text{Strong contacts : } f_n^c > \xi \bar{F} \quad (1)$$

Here ξ is a dimensionless parameter through which a subset of contacts is identified.

* Tel.: +31 53 489 2528; fax: +31 53 489 3695.

E-mail address: n.p.kruyt@utwente.nl

Based on results of a two-dimensional computer simulation of the behaviour of a system of particles, Radjaï et al. (1998) noted that:

1. The shear stress of the granular material is largely determined by the contributions of the strong force network.
2. The direction of anisotropy of the weak contact network is perpendicular to the direction of anisotropy of the full contact network.
3. Interparticle friction is mostly activated at weak contacts. Although Radjaï et al. (1998) relate the mobilisation of friction directly to dissipation, such a relation is more complex (see Krut and Rothenburg, 2006).

An objective of the current study is to provide an explanation of the first two findings, based on fairly weak assumptions that allow for analytical considerations.

Besides the strong and weak contact network of Radjaï et al. (1998), alternative contact networks have been proposed (see for example Krut and Antony, 2007; Tordesillas and Muthuswamy, 2009; Hunt et al., 2010).

The overview of this study is as follows. The relevant basics of micromechanics of granular materials are summarised in Section 2. The first two findings of Radjaï et al. (1998) are explained within a statistical framework for the contact forces in Section 3. An alternative definition of weak and strong contact networks is proposed in Section 4. Finally, findings of this study are discussed in Section 5.

2. Micromechanics

For two particles p and q that are in contact, the vector from the centre of particle p to the centre of particle q is the branch vector \mathbf{l}^{pq} . The unit vector corresponding to the branch vector is the contact normal \mathbf{n}^{pq} . In the two-dimensional case considered here, the orientation θ^c of a contact c is the angle of the contact normal vector \mathbf{n}^c with respect to a reference direction.

Statistical properties of the contact orientations θ^c can be described by a fabric tensor (for example Satake, 1978; Kanatani, 1984) or by the contact distribution function $E(\theta)$ (Horne, 1965). The contact distribution function $E(\theta)$ gives the probability that for an arbitrary contact c its orientation θ^c lies in an interval of width $\Delta\theta$ around orientation θ

$$E(\theta)\Delta\theta = \text{Prob}\left[\theta - \frac{\Delta\theta}{2} < \theta^c < \theta + \frac{\Delta\theta}{2}\right] \quad (2)$$

The force exerted by particle q on particle p is denoted by \mathbf{f}^{pq} . In the two-dimensional case, the force vector \mathbf{f}^c at a contact c can be decomposed into scalar normal and tangential components, f_n^c and f_t^c respectively.

The expression for the average Cauchy stress tensor σ , in terms of contact force vectors \mathbf{f} and branch vectors \mathbf{l} , is given by (for example Drescher and de Josselin de Jong, 1972; Krut and Rothenburg, 1996)

$$\sigma_{ij} = \frac{1}{A} \sum_{c \in C} f_i^c l_j^c \quad (3)$$

where the summation is over contacts c in the set of contacts C that are present in the region of interest with area A (in the two-dimensional case considered here).

By grouping contacts with similar contact orientations, the discrete sum in Eq. (3) can be converted to an integral involving the contact distribution function $E(\theta)$ (Rothenburg and Bathurst, 1989)

$$\sigma_{ij} = m_A \int_0^{2\pi} E(\theta) \bar{f}_i(\theta) \bar{l}_j(\theta) d\theta \quad (4)$$

where $m_A = N_{\text{cont}}/A$ is the contact density (i.e. the number of contacts per unit area) and $\bar{\phi}(\theta)$ denotes the average of an arbitrary contact quantity ϕ^c over contacts with similar contact orientations θ .

Eq. (4) can be simplified by adopting two assumptions that have been verified by Rothenburg and Bathurst (1989). Firstly, it is assumed that the contact force vector \mathbf{f}^c and the branch vector \mathbf{l}^c are uncorrelated, i.e. $\bar{f}_i \bar{l}_j(\theta) \cong \bar{f}_i(\theta) \bar{l}_j(\theta)$. Secondly, for disk-shaped particles as considered here, the average branch vector is given by $\bar{l}_j(\theta) \cong \bar{D} n_j(\theta)$ where \bar{D} is the average particle diameter. With these assumptions, Eq. (4) can be simplified to

$$\sigma_{ij} = m_A \bar{D} \int_0^{2\pi} E(\theta) \bar{f}_i(\theta) n_j(\theta) d\theta \quad (5)$$

3. Analysis of findings by Radjaï et al. (1998)

The analysis by Radjaï et al. (1998) of the stress tensor σ is based on a division of the contact into weak and strong contacts, depending on the magnitude of the normal force f_n^c . Here this concept is formally described by a probability density function for the contact forces. To emphasise the main ideas and to allow for simple analytical developments, the contribution of the tangential forces f_t^c to the stress tensor is neglected here. Rothenburg and Bathurst (1989) have shown that the contribution of tangential forces to the macroscopic shear strength is not dominant.

The joint probability density function $P(f_n, \theta)$ describes the probability that for an arbitrary contact c its contact normal force f_n^c lies within an interval of width Δf_n around f_n and its contact orientation θ^c lies within an interval of width $\Delta\theta$ around θ . Thus

$$\text{Prob}\left[f_n - \frac{\Delta f_n}{2} < f_n^c < f_n + \frac{\Delta f_n}{2}, \theta - \frac{\Delta\theta}{2} < \theta^c < \theta + \frac{\Delta\theta}{2}\right] = P(f_n, \theta) \Delta f_n \Delta\theta \quad (6)$$

Alternatively, a conditional probability density function $P(f_n|\theta)$ can be defined that gives the conditional probability that for a contact c whose contact orientation θ^c lies within an interval of width $\Delta\theta$ around θ , its contact normal force f_n^c lies within an interval of width Δf_n around f_n . Thus

$$\text{Prob}\left[f_n - \frac{\Delta f_n}{2} < f_n^c < f_n + \frac{\Delta f_n}{2} \middle| \theta - \frac{\Delta\theta}{2} < \theta^c < \theta + \frac{\Delta\theta}{2}\right] = P(f_n|\theta) \Delta f_n \Delta\theta \quad (7)$$

The joint and conditional probability density functions, $P(f_n, \theta)$ and $P(f_n|\theta)$ respectively, are related by

$$P(f_n, \theta) = E(\theta) P(f_n|\theta) \quad (8)$$

Since $P(f_n|\theta)$ is a (conditional) probability density function, it must satisfy the normalisation condition for probabilities

$$1 = \int_0^\infty P(f_n|\theta) df_n \quad (9)$$

In terms of the conditional probability density function $P(f_n|\theta)$, the average normal force $\bar{f}_n(\theta)$ for contacts with orientation θ is given by

$$\bar{f}_n(\theta) = \int_0^\infty f_n P(f_n|\theta) df_n \quad (10)$$

The average, over all contacts, normal force \bar{F} is then given by

$$\bar{F} = \int_0^{2\pi} E(\theta) \bar{f}_n(\theta) d\theta \quad (11)$$

In biaxial and isobaric tests the contact distribution function $E(\theta)$ and the average normal force $\bar{f}_n(\theta)$ are well described by a

truncated Fourier series in contact orientation θ (Rothenburg and Bathurst, 1989)

$$E(\theta) \cong \frac{1}{2\pi} [1 + A_c \cos 2(\theta - \theta_0)] \quad (12)$$

$$\bar{f}_n(\theta) \cong f_0 [1 + A_n \cos 2(\theta - \theta_0)] \quad (13)$$

where A_c is the contact anisotropy, A_n is the normal force anisotropy, f_0 is a force amplitude and θ_0 is the angle of the major principal-stress direction with the reference direction. It follows from Eqs. (11) to (13) that the force amplitude f_0 is related to the contact-averaged force \bar{F} by

$$\bar{F} = f_0 \left[1 + \frac{1}{2} A_c A_n \right] \quad (14)$$

The first finding by Radjaï et al. (1998) listed in the Introduction on the contributions of the weak and the strong contacts to the macroscopic shear stress is explained theoretically in Section 3.1, while their second finding on the anisotropy of the weak contact network is predicted theoretically in Section 3.2.

3.1. Stress due to weak contacts

The stress tensor σ in Eq. (5) can be expressed in terms of the contact distribution function $E(\theta)$ and the conditional probability density function $P(f_n|\theta)$. Note that the contribution of tangential forces is neglected here, as explained at the beginning of Section 3. With this assumption, we obtain from Eqs. (5) and (10) that the total stress tensor σ is given by

$$\sigma_{ij} \cong m_A \bar{D} \int_0^{2\pi} E(\theta) n_i(\theta) n_j(\theta) \left\{ \underbrace{\int_0^\infty f_n P(f_n|\theta) df_n}_{\bar{f}_n(\theta)} \right\} d\theta \quad (15)$$

Similarly, the stress tensor s due to contributions of the weak contact network (i.e. those contacts for which $f_n^c \leq \xi \bar{F}$) is given by

$$s_{ij} \cong m_A \bar{D} \int_0^{2\pi} E(\theta) n_i(\theta) n_j(\theta) \left\{ \int_0^{\xi \bar{F}} f_n P(f_n|\theta) df_n \right\} d\theta \quad (16)$$

Note that the difference between the total stress σ in Eq. (15) and the ‘weak’ stress s in Eq. (16) lies in the upper limit in the integral over the normal forces f_n .

To evaluate the weak stress tensor s , an expression for the conditional probability density function $P(f_n|\theta)$ for the contact force is required. This distribution has been studied by Kruyt (2003) for anisotropic systems, from results of Discrete Element Methods simulations and theoretically using a maximum-entropy method. The assumption adopted here for $P(f_n|\theta)$ is based on the following considerations:

- Simplicity of the expression in order to emphasise the main ideas and to keep the analytical expressions tractable.
- Exponential decay of $P(f_n|\theta)$ with f_n for large f_n , as has been observed experimentally and in results of computer simulations (see for instance references given by Kruyt, 2003).
- Use of an expression involving only the average normal force $\bar{f}_n(\theta)$.
- Consistency with the normalisation condition for probabilities, Eq. (9), and with the expression for the average normal force $\bar{f}_n(\theta)$, Eq. (10).

A simple, self-similar expression for the conditional probability density function $P(f_n|\theta)$ that conforms to these considerations is given by the Gamma distribution

$$P(f_n|\theta) = \frac{r}{\Gamma(r)} \frac{1}{\bar{f}_n(\theta)} \left(\frac{f_n}{\bar{f}_n(\theta)} \right)^{r-1} e^{-r \frac{f_n}{\bar{f}_n(\theta)}} \quad (17)$$

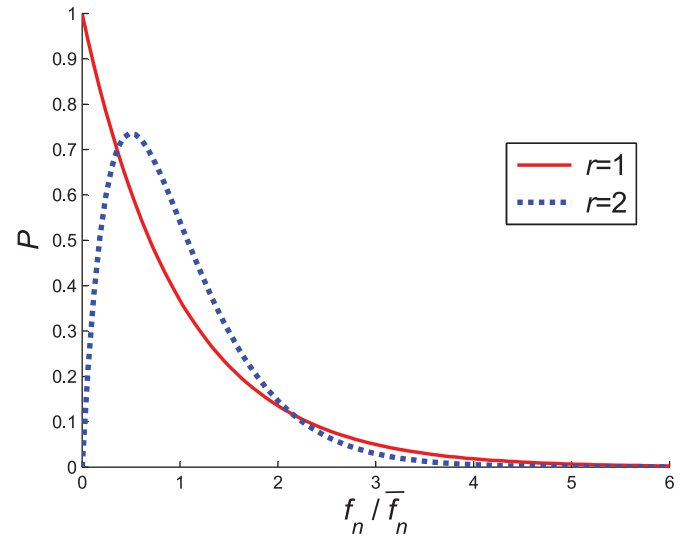


Fig. 1. Adopted Gamma distribution for the conditional probability density function $P(f_n|\theta)$ for $r = 1$ and $r = 2$; $\bar{f}_n = 1$.

Here r is a dimensionless shape factor, for which values of $r = 1$ and $r = 2$ are considered here. These probability density functions are shown in Fig. 1. For $r = 1$, the conditional probability density function $P(f_n|\theta)$ reduces to an exponential distribution. A theoretical argument leading to the value $r = 2$ is given by Kruyt and Rothenburg (2002).

This probability density function is self-similar in the sense that its shape is identical, relative to the average normal force $\bar{f}_n(\theta)$ for contacts with orientation θ . By employing more detailed and complex expressions for the conditional probability density function $P(f_n|\theta)$, better quantitative agreement with results from DEM simulations may be obtained. However, it is considered that the qualitative agreement is not affected.

The major and minor principal values of the average stress tensor σ are denoted by σ_1 and σ_2 , respectively, while those of the weak stress tensor s are denoted by s_1 and s_2 , respectively.

It follows from Eqs. (12), (13) and (15), after some algebra in which a linearisation is performed with respect to A_c and A_n , that the shear strength $(\sigma_1 - \sigma_2)/(\sigma_1 + \sigma_2)$ of the system due to all contacts is given by

$$\frac{\sigma_1 - \sigma_2}{\sigma_1 + \sigma_2} \cong \frac{1}{2} [A_c + A_n] \quad (18)$$

This is (of course) equivalent to the stress–force–fabric relationship obtained by Rothenburg and Bathurst (1989), considering that the contribution of tangential forces has been neglected here.

The weak stress tensor s can be obtained in an analogous manner from Eqs. (12), (13), (16) and (17). The results for the weak stress s are given here relative to the total stress σ . The relative pressure $(s_1 + s_2)/(\sigma_1 + \sigma_2)$ and the relative shear stress $(s_1 - s_2)/(\sigma_1 - \sigma_2)$ are given by

$$\begin{aligned} \frac{s_1 + s_2}{\sigma_1 + \sigma_2} &\cong 1 - [1 + \xi F(\xi)] e^{-r\xi} \\ \frac{s_1 - s_2}{\sigma_1 - \sigma_2} &\cong \frac{s_1 + s_2}{\sigma_1 + \sigma_2} - \frac{A_n}{A_n + A_c} G(\xi) e^{-r\xi} \end{aligned} \quad (19)$$

where $F(\xi)$ and $G(\xi)$ are given by (for the cases of $r = 1$ and $r = 2$ that are considered here)

$$F(\xi) = r + 2(r - 1)\xi \quad G(\xi) = r^2 \xi^{r+1} \quad (20)$$

Note that as $\xi \rightarrow \infty$, $(s_1 + s_2)/(\sigma_1 + \sigma_2) \rightarrow 1$ and $(s_1 - s_2)/(\sigma_1 - \sigma_2) \rightarrow 1$, since the weak contact network becomes identical to the total contact network as $\xi \rightarrow \infty$.

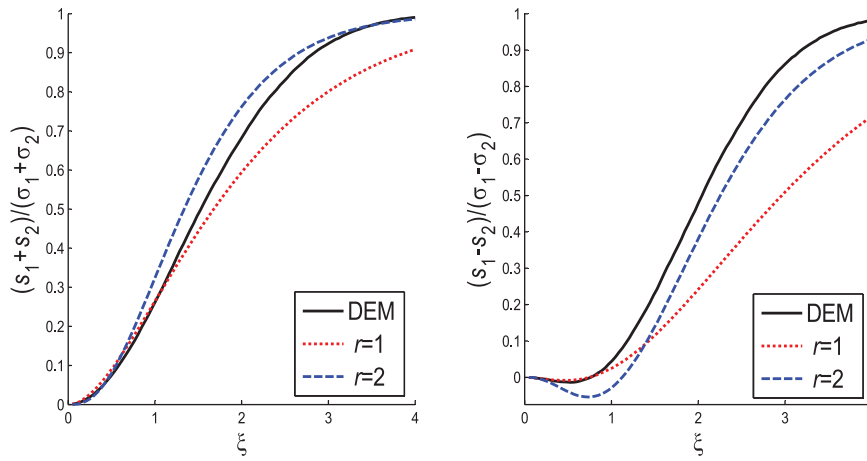


Fig. 2. Comparison of results from a DEM simulation and the current theory, Eq. (19), for $r = 1$ and $r = 2$. Left: pressure $(s_1 + s_2)/2$ of weak contacts, relative to pressure $(\sigma_1 + \sigma_2)/2$ of full contact network. Right: shear stress $(s_1 - s_2)/2$ of weak contacts, relative to shear stress $(\sigma_1 - \sigma_2)/2$ of full contact network.

The theoretical predictions in Eq. (19) are compared to results from a Discrete Element Method simulation (as proposed by Cundall and Strack, 1979; DEM for short) for a state with peak shear-strength for a system with interparticle friction coefficient $\mu = 0.5$. A detailed description of this DEM simulation is given by Krut and Rothenburg (2014). This comparison is shown in Fig. 2. The results from the DEM simulation show that at $\xi = 1$ the weak contacts contribute about 27% to the total pressure (see Fig. 2, left), while they contribute 5% to the shear stress (see Fig. 2, right). As emphasised by Radjai et al. (1998), this means that the contribution of the weak contacts to the shear stress is small. Hence, the shear stress is mainly carried by the strong contact network.

There is qualitative agreement between the results of the DEM simulation and the theoretical prediction, Eq. (19). In particular, the current simple theory predicts that $(s_1 - s_2)/(\sigma_1 - \sigma_2)$ is significantly smaller than $(s_1 + s_2)/(\sigma_1 + \sigma_2)$ for small values of ξ (for $r = 1$ and $\xi = 1$, the weak contacts contribute about 27% to the total pressure, while they contribute 3% to the shear stress; for $r = 2$ and $\xi = 1$, the corresponding values are 33% and -3% , respectively). Quantitatively, the theory underpredicts the contribution of the weak contact network to the shear strength, both for $r = 1$ and $r = 2$.

In short, the presented theory gives a qualitative explanation of the first finding of Radjai et al. (1998) as listed in the Introduction.

3.2. Contact distribution function of weak contacts

The contact distribution function $e(\theta; \xi)$ for weak contacts is defined in a manner analogous to the definition in Eq. (2) of the contact distribution function $E(\theta)$ for all contacts. The contact distribution function $e(\theta; \xi)$ gives the conditional probability that an arbitrary weak contact c (for which $f_n^c \leq \xi \bar{F}$) has an orientation θ^c that lies in an interval of width $\Delta\theta$ around orientation θ . Thus

$$e(\theta; \xi) \Delta\theta = \text{Prob} \left[\theta - \frac{\Delta\theta}{2} < \theta^c < \theta + \frac{\Delta\theta}{2} \mid f_n^c \leq \xi \bar{F} \right] \\ = \frac{\text{Prob} \left[\theta - \frac{\Delta\theta}{2} < \theta^c < \theta + \frac{\Delta\theta}{2}, f_n^c \leq \xi \bar{F} \right]}{\text{Prob} [f_n^c \leq \xi \bar{F}]} \quad (21)$$

where the latter equality follows from the definition of conditional probability.

Based on its definition in Eq. (21), the contact distribution function $e(\theta; \xi)$ for weak contacts can be expressed in terms of the contact distribution function $E(\theta)$ for all contacts and the

conditional probability density for normal forces $P(f_n|\theta)$ as

$$e(\theta; \xi) = \frac{E(\theta) \int_0^{\xi \bar{F}} P(f_n|\theta) df_n}{\int_0^{2\pi} E(\theta') \int_0^{\xi \bar{F}} P(f_n|\theta') df_n d\theta'} \quad (22)$$

where Eq. (8) has been used.

Using Eqs. (12), (13), (17) and (22), it follows after some algebra involving linearisation with respect to A_c and A_n that the contact distribution function $e(\theta; \xi)$ for weak contacts has a similar structure to that given by Eq. (12) for the contact distribution function $E(\theta)$ for all contacts

$$e(\theta; \xi) \cong \frac{1}{2\pi} [1 + a_c \cos 2(\theta - \theta_0)] \quad (23)$$

and that the anisotropy $a_c(\xi)$ of the contact distribution function $e(\theta; \xi)$ for weak contacts is given by

$$a_c(\xi) \cong A_c - A_n H(\xi) \quad (24)$$

where $H(\xi)$ is given by

$$H = \begin{cases} r = 1 : & \frac{\xi}{e^\xi - 1} \\ r = 2 : & \frac{4\xi^2}{e^{2\xi} - 2\xi - 1} \end{cases} \quad (25)$$

According to Eq. (24), $a_c(\xi) \rightarrow A_c - rA_n$, as $\xi \rightarrow 0$ for weak contacts. This limit value may be negative. In this case the direction of anisotropy of the weak contact network is perpendicular to that of the full contact network.

Results for the anisotropy $a_c(\xi)$ of the contact distribution function $e(\theta; \xi)$ for weak contacts, as determined from the results of the DEM simulation, are compared to the theoretical prediction Eq. (24) in Fig. 3. This Figure shows qualitative agreement between the results of the DEM simulation and the theoretical predictions. In particular, the theory gives negative $a_c(\xi)$ for small values of ξ , as also observed in the results of the DEM simulation. For small values of ξ the magnitude of the anisotropy of the weak contact network is underpredicted by the theory with $r = 1$, while it is overpredicted for $r = 2$.

In short, the presented theory gives a qualitative explanation of the second finding of Radjai et al. (1998) as listed in the Introduction.

4. Alternative definition of strong and weak contacts

The definition in Eq. (1) of the weak and the strong contact network by Radjai et al. (1998) is based on the comparison of the contact force f_n^c with the contact-averaged force \bar{F} . This definition does not account for the direction-dependence of statistics,

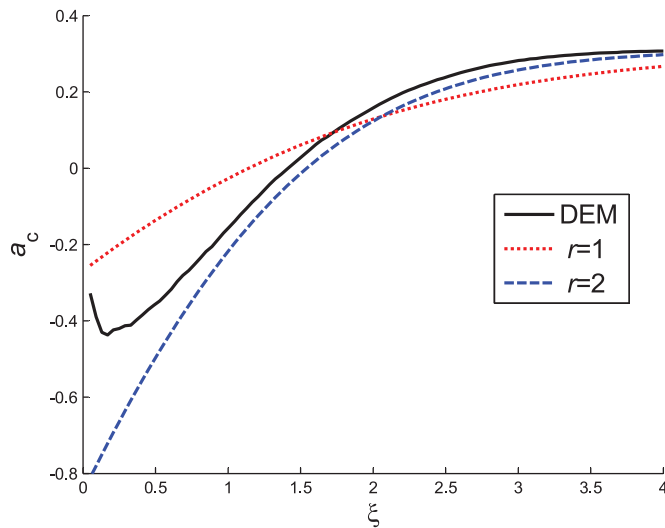


Fig. 3. Comparison of anisotropy $a_c(\xi)$ of the weak contact network. Results from a DEM simulation and according to the current theory, Eq. (24), for $r = 1$ and $r = 2$.

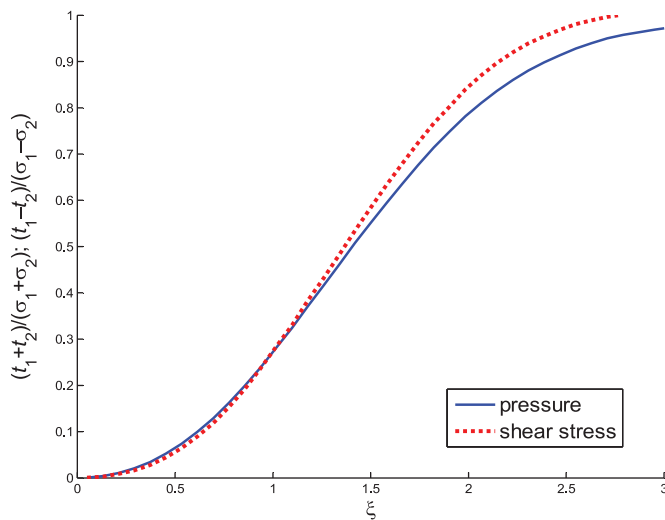


Fig. 4. Weak stresses \mathbf{t} according to alternative definition, Eq. (26), of the weak contact network. Results from a DEM simulation.

such as the average normal force $\bar{f}_n(\theta)$, of the contact forces (see Eq. (13)). An alternative definition of the weak and the strong contact network is proposed here where the contact force f_n^c is compared with the average force $\bar{f}_n(\theta^c)$ corresponding to the orientation θ^c of the contact. This leads to the following alternative definition of weak and strong contacts

$$\text{Weak contacts : } f_n^c \leq \xi \bar{f}_n(\theta^c) \quad \text{Strong contacts : } f_n^c > \xi \bar{f}_n(\theta^c) \quad (26)$$

The stress tensor $\mathbf{t}(\xi)$ that corresponds to this alternative definition of the weak contact network according to Eq. (26) has been computed from the results of the DEM simulation. Results are shown in Fig. 4. These results show that with this alternative definition of the weak and strong contact networks, that takes into account that the average normal forces $\bar{f}_n(\theta)$ are dependent on contact orientation θ , the difference in behaviour between pressure and shear stress of the weak stress tensor effectively disappears: shear stress and pressure are (almost) equally carried by the weak contacts.

The weak stress $\mathbf{t}(\xi)$ according to the alternative definition of weak and strong contacts according to Eq. (26) can be expressed

in terms of the conditional probability density $P(f_n|\theta)$ by (compare Eq. (16) for the expression of the weak stress according to the definition by Radjaï et al. (1998) of the weak and strong contact networks)

$$t_{ij} \cong m_A \bar{D} \int_0^{2\pi} E(\theta) n_i(\theta) n_j(\theta) \left\{ \int_0^{\xi \bar{f}_n(\theta)} f_n P(f_n|\theta) df_n \right\} d\theta \quad (27)$$

Note that the difference between the weak stress \mathbf{s} in Eq. (16) and the weak stress \mathbf{t} in Eq. (27) lies in the upper limit in the range of integration in the integral over the normal forces f_n .

The weak stress tensor \mathbf{t} can be obtained theoretically after some algebra, involving linearisation with respect to A_c and A_n , from Eqs. (12), (13), (17) and (27)

$$\frac{t_1 + t_2}{\sigma_1 + \sigma_2} = \frac{t_1 - t_2}{\sigma_1 - \sigma_2} \cong 1 - [1 + \xi F(\xi)] e^{-r\xi} \quad (28)$$

where $F(\xi)$ is given in Eq. (20).

According to the theoretical results in Eq. (28) there is no difference in behaviour between the pressure and the shear stress of the weak stress tensor: shear stress and pressure are equally carried by the weak contacts. This was also found from the result of the DEM simulation (see Fig. 4).

5. Discussion

Two findings by Radjaï et al. (1998) on the weak contact network have been analysed here. Their first finding is that weak contacts do not significantly contribute to the shear stress, while their second finding is that the direction of anisotropy of the weak contacts is perpendicular to that of the network consisting of all contacts.

In the current approach these findings are obtained through a statistical framework involving the conditional probability density function $P(f_n|\theta)$ for the contact forces, for which a simple self-similar expression has been assumed, Eq. (17). Based on this expression, the two findings by Radjaï et al. (1998) on the weak contact network are predicted theoretically in a qualitative sense. Improved quantitative agreement has not been pursued, as the emphasis is on the acquired understanding. For better quantitative agreement, the tangential forces need to be accounted for, as these currently have been neglected. In addition, more complex and realistic (in comparison with results from DEM simulations and experiments) expressions for the conditional probability density function $P(f_n|\theta)$ have to be adopted.

The definition by Radjaï et al. (1998) of the weak contact network is based on a comparison of the contact force f_n^c with a global average (over all contacts) force \bar{F} . As average forces are dependent on contact orientation, their (correct) analysis is biased in the sense that it does not consider this direction dependence. An alternative definition of the weak contact network has been proposed here, in which the contact force f_n^c is compared to the average normal forces corresponding to the contact orientation, $\bar{f}_n(\theta^c)$. With this definition, the pressure and the shear stress are (almost) equally carried by the weak contacts.

Force chains have been observed in experiments with photoelastic materials (for example de Josselin de Jong and Verruijt, 1969; Drescher and de Josselin de Jong, 1972). The contact forces in these chains are high. These force chains are generally aligned with the major principal stress. Since the contacts in these chains are adjacent, this means that there is a strong spatial correlation of the contact forces. Detailed micromechanical studies of such force chains have been performed (see for example Hunt et al., 2010; Tordesillas and Muthuswamy, 2009). These show that the stability of these force chains, with respect to buckling, is enhanced by the support of neighbouring particles with weak contacts. The use of the terminology of force chains is considered to be more descriptive

of stress transmission of granular materials in a qualitative sense (rather than the concept of weak and strong contact networks), as this terminology implies chains of particles with large, *spatially correlated* forces that are aligned with the major principal stress direction.

References

- Azéma, E., Radjaï, F., Dubois, F., 2013. Packings of irregular polyhedral particles: strength, structure, and effects of angularity. *Phys. Rev. E* 87, 062203.
- Biarez, J., Wiendieck, K., 1963. La comparaison qualitative entre l'anisotropie mécanique et l'anisotropie de structure des milieux pulvérulents. *C. R. Acad. Sci.* 256, 1217–1220.
- Cundall, P.A., Strack, O.D.L., 1979. A discrete numerical model for granular assemblies. *Géotechnique* 9, 47–65.
- Drescher, A., de Josselin de Jong, G., 1972. Photoelastic verification of a mechanical model for the flow of a granular materials. *J. Mech. Phys. Solids* 20, 337–351.
- Horne, M.R., 1965. The behaviour of an assembly of rotund, rigid, cohesionless particles, I and II. *Proc. R. Soc. Lond. A* 286, 62–97.
- Hunt, G.W., Tordesillas, A., Green, S.C., Shi, J.Y., 2010. Force-chain buckling in granular media: a structural mechanics perspective. *Philos. Trans. R. S. A – Math. Phys. Eng. Sci.* 368, 249–262.
- De Josselin de Jong, G., Verruijt, A., 1969. Étude photo-élastique d'un empilement de disques. *Cah. Groupe Fr. Rheol.* 2, 73–86.
- Kanatani, K., 1984. Distribution of directional data and fabric tensors. *Int. J. Eng. Sci.* 22, 149–164.
- Kruty, N.P., Rothenburg, L., 2002. Probability density functions of contact forces for cohesionless frictional granular materials. *Int. J. Solids Struct.* 39, 571–583.
- Kruty, N.P., 2003. Contact forces in anisotropic frictional granular materials. *Int. J. Solids Struct.* 40, 3537–3556.
- Kruty, N.P., Antony, S.J., 2007. On force, relative-displacement, and work networks in granular materials subjected to quasi-static deformation. *Phys. Rev. E* 75, 051308.
- Kruty, N.P., Rothenburg, L., 1996. Micromechanical definition of the strain tensor for granular materials. *J. Appl. Mech.* 63, 706–711.
- Kruty, N.P., Rothenburg, L., 2006. Shear strength, dilatancy, energy and dissipation in quasi-static deformation of granular materials. *J. Stat. Mech: Theory Exp.* P07021.
- Kruty, N.P., Rothenburg, L., 2014. On micromechanical characteristics of the critical state of two-dimensional granular materials. *Acta Mech.* 225, 2301–2318.
- Li, X., Yu, H.S., 2013. On the stress–force–fabric relationship for granular materials. *Int. J. Solids Struct.* 50, 1285–1302.
- Majmudar, T.S., Behringer, R.P., 2005. Contact force measurement and stress-induced anisotropy in granular materials. *Nature* 435, 1079–1082.
- Oda, M., 1972a. The mechanism of fabric change during compressional deformation of sand. *Soils Found.* 12, 1–18.
- Oda, M., 1972b. Initial fabric and their relation to mechanical properties of granular material. *Soils Found.* 12, 19–36.
- Oda, M., 1972c. Deformation mechanism of sand in triaxial compression tests. *Soils Found.* 12, 45–63.
- Ouadfel, H., Rothenburg, L., 2001. Stress–force–fabric relationship for assemblies of ellipsoids. *Mech. Mater.* 33, 201–221.
- Radjaï, F., Wolf, D.E., Jean, M., Moreau, J.J., 1998. Bimodal character of stress transmission in granular packings. *Phys. Rev. Lett.* 80, 61–64.
- Rothenburg, L., Bathurst, R.J., 1989. Analytical study of induced anisotropy in idealized granular materials. *Géotechnique* 39, 601–614.
- Satake, M., 1978. Constitution of mechanics of granular materials through graph theory. In: Cowin, S.C., Satake, M. (Eds.), *US-Japan Seminar on Continuum-Mechanical and Statistical Approaches to Granular Materials*. Elsevier, Amsterdam, The Netherlands, pp. 47–62.
- Tordesillas, A., Muthuswamy, M., 2009. On the modelling of confined buckling of force chains. *J. Mech. Phys. Solids* 57, 706–727.